Laser-Induced Reshaping of Metallodielectric Nanoshells under Femtosecond and Nanosecond Plasmon Resonant Illumination

Carla M. Aguirre,[†] Cristin E. Moran,[‡] James F. Young,[§] and Naomi J. Halas*[,‡,§]

Department of Physics and Astronomy, Department of Chemistry, Department of Electrical and Computer Engineering, and Rice Quantum Institute, Rice University, P.O. Box 1892, Houston, Texas 77005-1892

Received: July 29, 2003; In Final Form: March 2, 2004

Absorption of pulsed laser light energy at the plasmon resonant wavelength of silica−gold core−shell nanoparticles results in a reshaping of the nanoparticle's metal shell layer. Dramatically distinct and reproducible changes in nanoparticle morphology occur as a function of laser pulse width in the femtosecond versus nanosecond regime and laser fluence. The changes are accompanied by large modifications in the plasmon resonant wavelength and spectrum of the reshaped nanoparticle. At the highest femtosecond pulse energies used, deformation of the silica core is also observed.

Introduction

There is currently tremendous interest in developing controlled methods for producing nanostructures and nanoparticles of highly uniform size and shape in quantities sufficient to permit their use in applications. For metal nanostructures, this is motivated by an interest in controlling their optical properties, which are dominated by their plasmon response, since the plasmonic properties of metal nanostructures are determined by their size and shape. Recently, the fabrication of metallic and metallodielectric nanoparticles in a wide variety of shapes, such as rods,[1−3] triangles,[4] disks,[5,6] shells,[7−10] cups,[11,12] and cubes,[13] has been reported. The development of novel methods for the synthesis of entirely new nanostructures currently unattainable using standard chemical synthetic approaches is highly desirable, further expanding our current "toolbox" of nanoscale optically active structures.

One possible approach to the development of new metal-based nanostructures is the use of pulsed lasers to induce controlled heating of the nanostructures, which should lead to reshaping. Studies of the electron dynamics of metal nanoparticles have established that heat transfer from excited conduction electrons to the metal lattice after excitation by a laser pulse occurs in a few (2−5) picoseconds.[13−17] The lattice cools by transferring heat to the surrounding medium. The precise time scale for the heat dissipation to the embedding medium depends on the host's heat capacity, but in general is on the order of hundreds of picoseconds.[18] When the width of the excitation pulse is shorter than this time scale, it is possible to preferentially heat the metal lattice while the temperature of the surrounding medium remains unchanged. By using high-energy laser pulses, the temperature of metal nanoparticles can be raised by several hundred degrees.[19]

For all metal nanostructures regardless of initial shape, heating and melting by either thermal[20] or nonthermal sources will allow them to re-form to their most thermodynamically stable shape, that of a solid sphere. This metamorphosis can be monitored by the corresponding changes in the plasmon resonance frequency of the nanostructure. A number of studies have reported irreversible shape changes of metal nanoparticles that occur under the conditions of pulsed laser heating. Fragmentation and vaporization were reported for gold nanoparticles in aqueous solution under irradiation by high-energy pulses.[21−23] The melting of silver nanoparticles supported on a quartz substrate has also been studied.[24] The spherical metal nanoparticles used in these initial experiments were already in or close to their most thermodynamically favored shape. Subtle changes to their structure, and hence changes to their optical properties, were not readily observable. A series of interesting experiments conducted on gold nanorods have elucidated the possible mechanisms leading to the observed photoinduced modifications.[19,25,26] Because metal nanorods exhibit a distinct spectral response characteristic of their elongated shape, slight changes in morphology can be followed by observation of the optical signature of the irradiated product.

In this paper, we report a series of pulsed-laser-induced reshaping experiments on SiO_2−Au metallodielectric core−shell nanoparticles, known as nanoshells. The plasmon resonance of the nanoshell is a sensitive function of the relative dimensions of the core diameter and shell thickness, and can be tuned across much of the visible and infrared region of the spectrum by varying these dimensions. The unusually sensitive tunability of the metallic shell topology has generated significant recent theoretical interest in this nanostructure.[27−29] Since control of the far-field optical properties infers that the near-field properties are also precisely known, nanoshells provide a controlled electromagnetic nanoenvironment exploitable for Raman and SPR-based chemical sensing applications.[30−32] The photothermal effects of nanoshells are typically very strong and have been exploited in applications, such as optically addressable nanoshell−polymer composites for drug delivery.[33] Tuning the plasmon resonance into the near-infrared region of highest physiological transmissivity has led to a variety of nanoshell-based biotechnological innovations, such as a whole blood immunoassay[34] and photothermally induced cell necrosis in vitro.[35]

The series of pulsed laser irradiation experiments on Au nanoshells reported here is, to our knowledge, the first pulsed laser reshaping study of a metal/dielectric composite nanostruc-

* To whom correspondence should be addressed. E-mail: halas@rice.edu.
[†] Department of Physics and Astronomy.
[‡] Department of Chemistry.
[§] Department of Electrical and Computer Engineering.

10.1021/jp036222b CCC: $27.50
Published on Web 05/01/2004

ture. In comparison with laser-induced reshaping of nanorods, the different geometry and most importantly the presence of a silica core result in a variety of different morphologies of the reshaped nanostructures. This reshaping is dramatically dependent both on laser power and on laser pulse width, where each regime yields distinct and different reshaped nanoparticle morphologies dependent on the degree of laser heating and the thermalization dynamics. By controlling the precise heating conditions, it was possible to control the morphology of the final irradiated product. Unlike gold nanorods, the gold nanoshell extinction spectrum does not overlap that of gold nanospheres, providing us with increased observational sensitivity to the production of gold nanospheres from exposure to high-energy laser pulses. To compare our results directly to those of previous studies, we used an experimental setup similar to that of the nanorod studies. In this way, we investigated the laser-induced shape changes of gold nanoshells as a function of laser pulse width and pulse energy. Another characteristic unique to Au nanoshells is the polycrystalline structure of the metal layer, which makes them sensitive to melting along surface defects. We determined that the melting threshold of a nanoshell using femtosecond pulses can be estimated using the bulk properties of gold. The slow deformation and reshaping of gold nanoshells occurs below this threshold by heating over many pulses. Destruction of gold nanoshells from nanosecond pulses occurs at pulse energies approximately 4 times the energy of femtosecond pulses. We have also confirmed that the use of femtosecond pulses leads to a much more efficient and controllable heating regime compared to the use of nanosecond pulses.

Experimental Section

Gold Nanoshell Fabrication. Nanoshells having dipolar plasmon resonances at the working frequencies of both our nanosecond and femtosecond lasers were fabricated following a previously reported method.[7] Briefly, monodisperse silica nanospheres were fabricated via the Stöber method.[36] The surface of these nanoparticles was terminated with an organosilane molecule [(3-aminopropyl)triethoxysilane]. Small (2−3 nm) gold nanoparticles were fabricated following a method described by Duff et al.[37] and then attached to the silica nanoparticles through the interaction with the amine group of the organosilane linkage molecule. Finally, the growth and coalescence of the immobilized seed particles into a complete metal shell proceeded through the reduction of a mixture of chloroauric acid and potassium carbonate by a 29% solution of formaldehyde. The samples were washed through multiple steps of centrifugation and redispersion in ultrapure water (Millipore, Milli-Q). Scanning electron microscopy (SEM) images of both the silica nanospheres and the final nanoshell particles were obtained using a JEOL 6500 field emission scanning electron microscope. The size and distribution of our samples were determined by measuring at least 300 particles. The nanoshell solution having a peak absorbance at 800 nm (sample A) consisted of particles with a 62 ± 5 nm radius silica core and a 12 ± 1 nm gold shell (Figure 1a,b). The second solution with a peak absorbance at 1064 nm (sample B) consisted of nanoshells with a 110 ± 12 nm radius silica core and a 12 ± 1 nm metal shell (Figure 1c,d). It was possible to determine the particle concentration from the calculated value of the extinction cross-section (calculated using Mie scattering theory) and the experimental extinction spectrum as determined by UV−vis spectroscopy using a Varian Cary 5000 spectrometer.

Irradiation Experiments. The irradiation experiments were carried out using two separate laser systems. For the femtosecond irradiation experiments we used pulses generated by a Ti:sapphire regenerative amplifier (Coherent Rega 9000) seeded by pulses from a Kerr lens mode-locked femtosecond Ti:sapphire laser (Coherent Mira 900). This system delivers pulses of 200 fs in duration at a 250 kHz repetition rate at energies of up to 2.8 μJ per pulse. The nanosecond laser used was a Q-switched Nd:Yag laser delivering 9 ns pulses at a repetition rate that can be varied from 10 Hz to single-pulse capability. The energy was varied using a variable filter, and the beam was focused at the sample. For both the femtosecond and nanosecond irradiation experiments, 250 μL of the respective nanoshell solutions was irradiated inside a rotating 1 mm path length cylindrical quartz cell. The cell was rotated at a minimum of 1000 rpm to ensure proper mixing conditions. To facilitate mixing, 2 parts acetone was added to 1 part original nanoshell solutions. The concentration of particles in the irradiated solution was 6.45×10^9 particles/mL for sample A and 6.78×10^8 particles/mL for sample B.

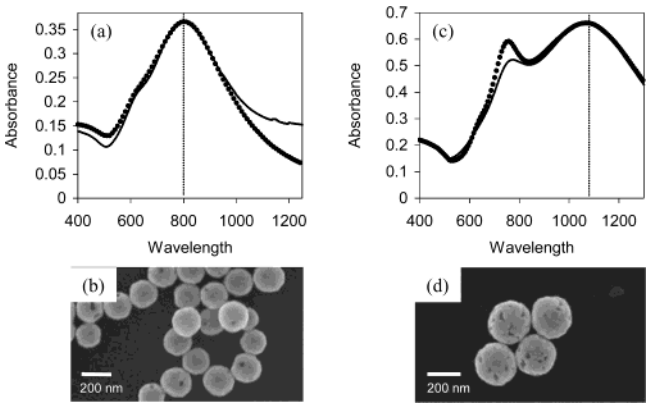

Figure 1. Measured UV−vis extinction spectra (solid lines) and theoretical fit (dotted lines) of aqueous solutions of gold nanoshells resonant at the working frequencies of both the (a) femtosecond (800 nm) and (c) nanosecond (1064 nm) lasers. Corresponding SEM images of gold nanoshells having (b) a 62 ± 5 nm radius silica core and a 12 ± 1 nm gold shell and (d) a 110 ± 12 nm radius silica core and a 12 ± 1 nm metal shell.

The irradiation products of the nanoshell solutions after exposure to laser pulses of varying energies and irradiation times were characterized using UV−vis spectroscopy, transmission electron microscopy (TEM) (JEOL 2010x), and scanning electron microscopy. All the spectra shown were recorded in a 10 mm path length quartz cuvette immediately after irradiation.

Results and Discussion

Femtosecond Irradiation. Gold nanoshells (sample A) were irradiated by laser pulses with wavelengths close to their absorption maxima. A series of experiments were conducted by varying both the pulse energy and irradiation time. Because the specific irradiation conditions are also a function of the laser spot size, particle dimensions, particle concentration, and mixing conditions, these parameters are held constant, and the irradiation time and pulse energy are varied independently. The laser spot size used in this set of experiments was measured by scanning a knife edge and fitting the intensity profile of the laser beam to a Gaussian distribution function. The beam diameter was determined to be 84 ± 5 μm. The intensity of the laser pulse was varied from 0.2 to 2.8 μJ by using a variable filter. Our results for the femtosecond irradiation of gold nanoshells in solution are summarized in Figure 2. The UV−vis extinction spectra (Figure 2a,c,e) and images of the final irradiation products after the longest irradiation times (Figure 2b,d,f) for a given laser pulse intensity are shown.

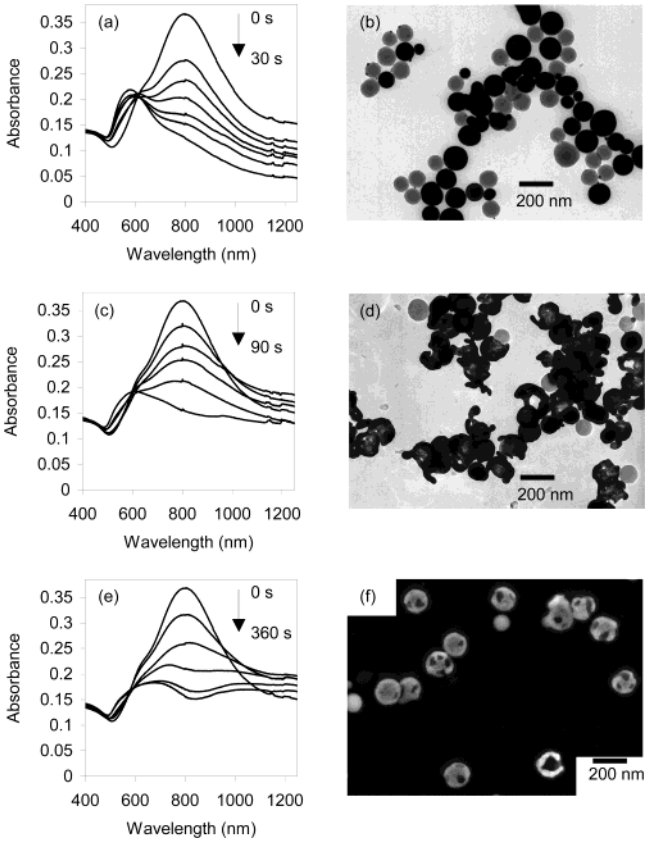

Figure 2. UV−vis extinction spectra and corresponding micrographs of a gold nanoshell solution after exposure to 800 nm femtosecond pulses. The energy of the pulses is varied from a high-irradiation regime of 2.8 μJ (a, b) to an intermediate-irradiation regime of 0.37 μJ (c, d) and a low-irradiation regime of 0.28 μJ (e, f). Each panel (a, c, e) illustrates the evolution of the extinction spectra with increasing irradiation times. To the right of the extinction spectra are TEM (b, d) and SEM (f) micrographs of the final irradiation products corresponding to different total irradiation times. The scale bar is 200 nm for each micrograph.

The evolution of the extinction spectrum of a nanoshell solution with increasing irradiation times at a pulse energy of 2.8 μJ is shown in Figure 2a. After short irradiation times, the amplitude of the absorption band at 800 nm decreases and we observe the emergence of a new absorption peak at 577 nm. After irradiation for 30 s (7.5×10^6 laser shots), the original nanoshell plasmon feature disappeared, leaving only the absorption band at 577 nm, characteristic of large spherical gold nanoparticles. TEM images taken of the final irradiation product (Figure 2b) confirm that the nanoshells in the original solution have been destroyed and that only bare silica particles and gold nanospheres remain. The average diameter of the solid gold nanoparticles as determined from TEM is 53 ± 10 nm, which is equivalent to the volume of the original gold shell. This indicates that each gold nanoparticle is the remains of a single gold shell. At this point all the nanoshells in the 250 μL solution have been exposed to at least a single pulse and have been completely destroyed. Under a 2.8 μJ irradiation, the metal shell does not fragment into smaller particles, but deforms by melting into a solid gold particle.

Upon closer inspection of the TEM images (Figure 3) we also observed the partial, localized deformation of the silica core. This is surprising given that we are well below (approximately 50×) the reported threshold for damage of silica by femtosecond laser pulses,[38] inferring that the reshaping of the silica may be a plasmon-assisted process. The melting trend for the metal shell

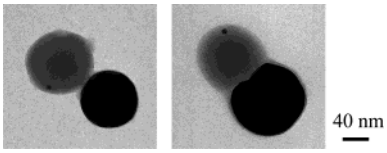

Figure 3. Two representative TEM images illustrating the deformation of the silica core of a gold nanoshell by femtosecond pulses in the high-irradiation regime (2.8 μJ). In each image the silica core has been deformed near the point of contact to the melted gold shell. In the image on the right the melted core has re-formed around part of the gold particle. This indicates high-intensity localized heating due to irradiation at the plasmon resonant wavelength. The scale bar is 40 nm for both micrographs.

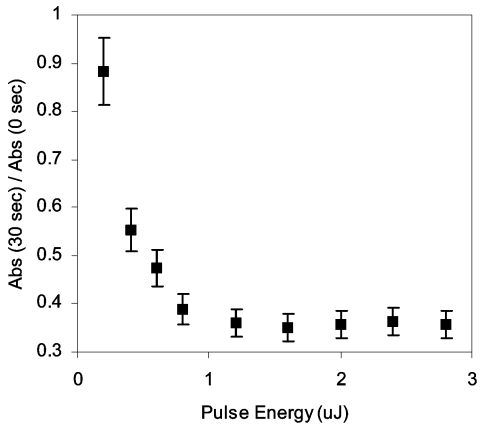

Figure 4. Intensity of the 800 nm absorption band of irradiated gold nanoshells after a 30 s irradiation cycle (7.5×10^6 laser shots) as a function of femtosecond laser pulse energy (2.8−0.2 μJ). A threshold between partial destruction (<1.2 μJ) and total melting of all the nanoshells in solution (>1.2 μJ) is seen. The result was normalized to the nonirradiated solution absorption value.

was observed at irradiation energies greater than 1.2 μJ, but the reshaping and deformation of the silica core was observed only for the highest pulse intensities (>2.4 μJ). At this high-intensity regime we believe that the heat dissipated to the silica core could be sufficient to locally raise its temperature above the melting point. However, other energy-dissipating mechanisms such as the excitation of coherent phonons may also play some role.[39]

Previous studies on gold nanorods have determined the threshold for complete melting of all the metal nanoparticles in the irradiation volume by monitoring the evolution of the extinction spectrum over time.[26] We used a similar approach to determine the melting threshold of a gold nanoshell. We performed a set of experiments in which we examined the magnitude of the absorption band at 800 nm after a 30 s exposure to pulses of different energies. As discussed previously, a 30 s exposure is the shortest irradiation time (smallest number of laser shots) necessary for all nanoparticles in the cylindrical cell to be exposed to at least a single laser pulse. Figure 4 plots the relative magnitude of the absorption peak as a function of the pulse energy. Each point is the average of four irradiation cycles for each given pulse energy. We can identify a clear transition from a regime where a 30 s exposure leads to the complete destruction of all the nanoshells in solution to a regime where the nanoshells have been only partially destroyed. In this way, we determined that the threshold for complete melting of all nanoshells in the irradiation volume over a single pulse is 1.2 μJ.

As parts d and f of Figure 1 illustrate, at energies below the 1.2 μJ threshold, the gold shell of the nanoparticles no longer completely melts over a single pulse but reshapes with succes-

sive pulses. In addition, the spectral response of the reshaped nanoshell is shifted away from the irradiation wavelength. Unlike gold nanorods, the line width of the nanoshell plasmon band is not primarily the result of inhomogeneous broadening due to the size distribution in the solution of particles. Rather, it is predominantly due to homogeneous broadening resulting both from finite size effects and from increased electron interface scattering at the crystalline domains and interfaces of the metallic shell.[40] The polycrystalline structure of the metallic shell is inherent from the colloid-nucleated growth of the fabrication process. Therefore, in these experiments all the nanoshells in the irradiated volume absorb essentially the same energy from a given pulse. The low-energy irradiation by femtosecond pulses results in a slow reshaping of *all* the nanoshells in solution. At the intermediate pulse energy of 0.37 μJ we observe the partial melting of the gold nanoshell over successive pulses (Figure 2d). The gold shell opens, releasing the silica core. At the lowest pulse intensity (0.28 μJ) we observe the burning of an optical hole in the absorption spectrum (Figure 2e). From inspection of the SEM image of the irradiated product (Figure 2f) we observe the partial reshaping of the metal shell that has remained on the silica core. Large holes have opened on the originally smooth gold nanoshell surface. This reshaping likely initiates along the defects of the polycrystalline metal shell due to the temperature rise. In summary, by using femtosecond pulses, it is possible to melt the nanoparticles very efficiently over a single pulse with high laser energies. It is also possible to reshape the metal shell slowly using pulses below the melting threshold.

Nanosecond Experiments. Two different irradiation experiments were conducted on gold nanoshells resonant at 1064 nm using a Nd:Yag nanosecond laser. The first determined the threshold for destruction of a nanoshell over a single pulse, and the second studied the shape transformations as a result of both high (single pulse) and low (many pulses) irradiation conditions.

The threshold for the destruction of gold nanoshells by a single nanosecond laser shot was determined by irradiating a small (25 μL) volume of sample B inside a stationary 1 mm path length quartz cuvette. Mixing was not needed since we were exposing the solution to a single laser shot. The laser spot of our nanosecond laser was measured using a knife edge, was determined to be approximately 3 ± 0.5 mm, and was chosen to span most of the 25 μL volume. At high pulse energies, exposure to a single laser shot results in the destruction of the metal nanoshells observed by the decrease of the absorption band at 1064 nm and the appearance of a peak at 530 nm. The amplitude of the peak at 530 nm after irradiation by a single nanosecond pulse was measured and is plotted as a function of pulse intensities in Figure 5.

Unlike the femtosecond regime, there is not a sharp threshold for the destruction of nanoshells by a single nanosecond laser pulse. This result can be explained by the simultaneous fragmenting and melting of the nanoparticles in the irradiation volume. It has been proposed that, for nanosecond pulses, photofragmentation is responsible for the destruction of metal nanoparticles. Previous studies have suggested that photofragmentation is the result of multiphoton ionization.[21] The ejection of electrons by an energetic laser pulse can cause the particles to become positively charged. The particles then fragment due to Coulomb repulsion. Other groups have proposed that photofragmentation occurs when the molten lattice is continuously heated over long laser pulses.[19] This leads to high-density gradients within the metal particle, causing the ablation of the metal. In our experiment, as the energy of the pulse decreases the destruction of the metal shell through photofragmentation

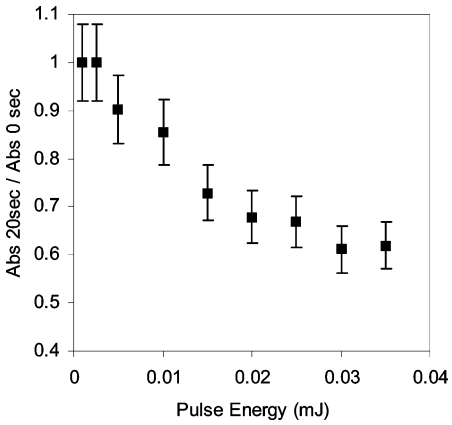

Figure 5. Intensity of the 530 nm absorption band of a nanoshell solution after exposure to a single nanosecond laser shot as a function of laser pulse energy (0.001−0.035 mJ). At energies below 0.005 mJ no colloidal gold nanoparticles are produced after illumination by a single pulse. Above this threshold, there is an increase in the number of nanoparticles produced at higher energies as the efficiency of the photofragmentation process increases. The result was normalized to the nonirradiated solution absorption value.

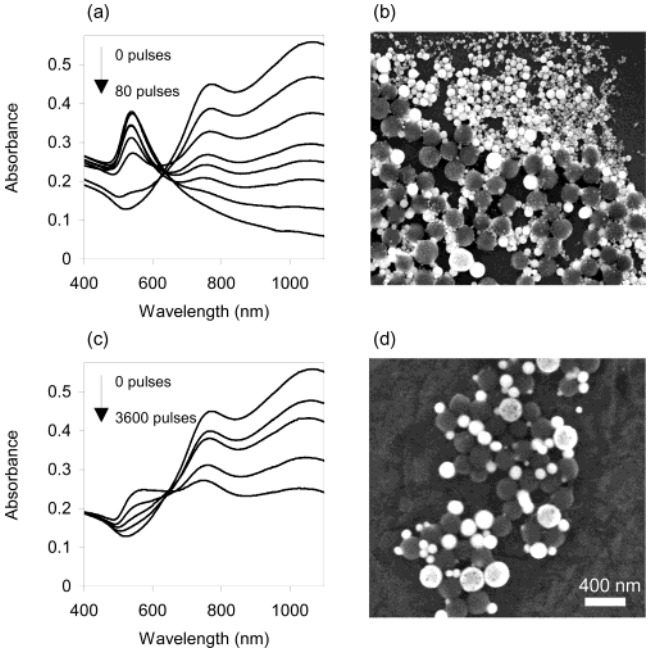

Figure 6. Spectral evolution and morphological changes of gold nanoshells in solution after exposure to 1064 nm nanosecond pulses. Irradiation energies were varied from a high-irradiation regime of 0.035 mJ (a, b) to a low-irradiation regime of 0.001 mJ (c, d). In the high-irradiation regime the gradual disappearance of the nanoshell spectrum, and the appearance of the solid gold nanoparticle plasmon at 520 nm, is seen. In the low-irradiation regime the spectral changes are much slower, but the production of gold colloid is still observed. SEM images correspond to the final irradiation product after (b) 80 and (d) 3600 pulses. The scale bar is 400 nm in both micrographs.

becomes less efficient, leading to a smaller yield in colloidal nanoparticles. At energies below 0.005 mJ, we no longer observe the production of colloidal gold nanoparticles after exposure to a single pulse. Below this threshold value, the heating of the metal by a single nanosecond laser pulse does not lead to the complete destruction of the gold nanoshells.

The results for irradiations at both the high- and low-energy limits used for this experiment are shown in Figure 6. The rotating cylindrical cell setup was used for this set of experiments. As mentioned above, at high energies (0.035 mJ) the

nanoshells fragment into small metal colloids (Figure 6a,b) over a single laser shot. The gold particles produced are spherical and have a broad size distribution. The size of the smallest nanoparticles produced is only ~1−3 nm. This is in contrast to the production of large spherical nanoparticles observed for femtosecond pulses. The results for irradiation at the low-energy limit (0.001 mJ) of our experiment can be seen in Figure 6c,d. Below this energy no spectral change was observed even for very long irradiation times. In this low-intensity heating regime the absorption of many nanosecond pulses does lead eventually to the production of colloidal gold nanoparticles. Previous studies on the thermal stability of gold nanoshells have determined that the simultaneous heating of the nanoparticle and the surrounding medium leads to the destruction of the metal shell and the production of colloidal gold nanoparticles.[20] Because heat transfer to the surrounding medium occurs over the width of the pulse, irradiation by long nanosecond laser pulses is analogous to this heating regime. It was not possible to observe either the slow reshaping of the metal shell or the burning of a spectral hole in the absorbance data for gold nanoshells.

Determination of the Lattice Temperature Rise. To better understand the mechanisms leading to the reshaping of metal nanoshells, we have estimated the lattice temperature for the different irradiation regimes. The heating of the lattice by a femtosecond pulse happens a few picoseconds after the absorption of the energy by the conduction electrons of the metal shell. During the absorption process the physical properties of the nanoparticle remain unchanged from their initial values. Using the approach taken by Link et al.,[26] it is possible to calculate the fraction of energy each particle absorbs (E_{abs}) from the absorbance value of the unexposed nanoparticle solution and the concentration of nanoparticles in solution. Using this value for E_{abs}, the mass of the metallic gold shell (m), and the bulk values of the thermal capacity (c) and the heat of melting (H), the temperature of the metallic shell lattice is given by the thermodynamic relations

$$T = \frac{E_{abs}}{mc} + 293 \quad (1)$$

$$T = \frac{E_{abs} - H}{mc} + 293 \quad (2)$$

Equation 1 is for temperatures below the melting temperature of gold, while eq 2 is for temperatures above this value. The results are plotted in Figure 7 as a function of laser pulse energy. The values for the lattice temperature agree remarkably well with our irradiation data. The threshold for complete destruction of a gold nanoshell by femtosecond pulses (1.2 μJ) correlates with a lattice temperature of 1064 °C, the melting point of bulk gold. For lattice temperatures below this value the destruction of the metal shell is the result of heating-induced reshaping of the metallic shell to a more thermodynamically stable morphology.

This calculation is not applicable to nanosecond pulses. Because the energy absorption by the metal and heat transfer to the surrounding medium occur simultaneously, it is impossible to determine the temperature increase following this procedure. However, the threshold for complete destruction of gold nanoshells by nanosecond laser pulses is only 4 times that by femtosecond laser pulses. At the highest femtosecond pulse energies used the lattice temperature was calculated to be ~2400 °C. Because the highest pulse energy used for our nanosecond laser experiments is 10 times this value, it is possible that irradiation by high-energy nanosecond laser pulses leads to the vaporization of the metal shell and production of metal nanoparticles having a broad size distribution.

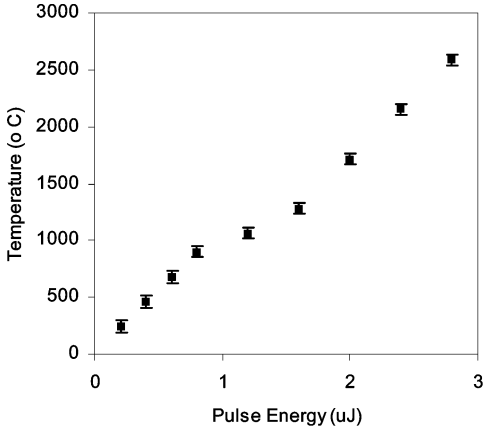

Figure 7. Calculated gold shell temperature after exposure to femtosecond laser pulses as a function of laser pulse energy. At a pulse energy of 1.2 μJ a plateau indicates a phase transition and melting of the nanoshells at 1064 °C, the melting point of bulk gold.

Conclusion

When nanoshells are irradiated by short laser pulses, the absorbed energy is efficiently converted to heat and the nanoshells reshape due to the increase of the lattice temperature. Unlike gold nanorods, the shape of gold nanoshells is not stabilized by surfactant capping molecules. The shape of the irradiated product is, in the case of our studies, not influenced by the high-temperature stability of this capping layer.[41] The precise final morphology of gold nanoshells after pulsed laser irradiation is a function of both the energy and the width of the excitation pulses. Intense irradiation by femtosecond pulses leads to the complete melting of the metallic shell over a single pulse. The gold reshapes, forming a large, gold nanosphere. In contrast to gold nanorods, the initial nanoparticle is neither a solid metal particle nor a single crystal, demonstrating that this shape transformation is a general result for femtosecond heating of metal nanoparticles. At this irradiation regime it was also observed that the silica core of the gold nanoshell undergoes localized deformation at the dielectric/metal interface, an effect which to our knowledge has not been previously reported. For lower pulse energies, slow reshaping of the metallic shell was accomplished by irradiation of gold nanoshells over several successive femtosecond pulses. This leads to the transformation of all the irradiated nanoshells into deformed or partially melted gold shells. The deformation is believed to originate at the defects of the metallic gold shell. In contrast, it was found that irradiating nanoshells using nanosecond pulses always led to the production of colloidal gold nanoparticles. The careful and controlled reshaping of gold nanoshells observed by femtosecond laser irradiation was not possible with nanosecond pulses. Intense irradiation by nanosecond pulses leads to the fragmentation of the gold shell and production of small colloidal gold nanoparticles with a large size distribution. Finally, it was estimated that the lattice temperature could be raised to several thousand degrees by femtosecond laser irradiation. The rapid and localized temperature rise of the metal lattice could prove useful in biomedical applications.[42,43]

Acknowledgment. N.J.H. gratefully acknowledges helpful discussions with S. Link concerning sample cell design, and we acknowledge the Army Research Office, the Air Force Office

of Scientific Research, the Robert A. Welch Foundation, NASA, and the National Science Foundation for support.

References and Notes

(1) Jana, N. R.; Gearheart, L.; Murphy, C. J. *J. Phys. Chem. B* **2001**, *105*, 4065.
(2) Nicewarner-Pena, S. R.; Griffith-Freeman, R.; Reiss, B. D.; He, L.; Pena, D. J.; Walton, I. D.; Cromer, R.; Keating, C. D.; Natan, M. J. *Science* **2001**, *294*, 137−141.
(3) Nikoobakht, B.; El-Sayed, M. A. *Chem. Mater.* **2003**, *15*, 1957−1962.
(4) Jensen, T. R.; Schatz, G. C.; Van Duyne, R. P. *J. Phys. Chem. B* **1999**, *103*, 2394−2401.
(5) Chen, S.; Fan, Z.; Carroll, D. L. *J. Phys. Chem. B* **2002**, *106*, 10777−10781.
(6) Maillard, M.; Giorgio, S.; Pileni, M. P. *J. Phys. Chem. B* **2003**, *107*, 2466−2470.
(7) Oldenburg, S. J.; Averitt, R. D.; Westcott, S. L.; Halas, N. J. *Chem. Phys. Lett.* **1998**, *288*, 243−247.
(8) Jackson, J. B.; Halas, N. J. *J. Phys. Chem. B* **2001**, *105*, 2743.
(9) Graf, C.; van Blaaderen, A. *Langmuir* **2002**, *18*, 524−534.
(10) Kobayashi, Y.; Salgueirina-Maceira, V.; Liz-Marzan, L. M. *Chem. Mater.* **2001**, *13*, 1630−1633.
(11) Love, J. C.; Gates, B. D.; Wolfe, D. B.; Paul, K. E.; Whitesides, G. M. *Nano Lett.* **2002**, *2*, 891−894.
(12) Charnay, C.; Lee, A.; Man, S. Q.; Moran, C. E.; Radloff, C.; Bradley, R. K.; Halas, N. J. *J. Phys. Chem. B* **2003**, *107*, 7327−7333.
(13) Sun, C. K.; Vallee, F.; Acioli, L. H.; Ippen, E. P.; Fujimoto, J. G. *Phys. Rev. B* **1994**, *50*, 15337−15348.
(14) Del Fatti, N.; Voisin, C.; Achermann, M.; Tzortzakis, S.; Christofilos, D.; Vallee, F. *Phys. Rev. B* **2000**, *61*, 16956−16966.
(15) Groeneveld, R. H. M.; Sprik, R.; Lagendijk, A. *Phys. Rev. B* **1995**, *51*, 11433−11445.
(16) Klar, T.; Perner, M.; Grosse, S.; von Plessen, G.; Spirkl, W.; Feldmann, J. *Phys. Rev. Lett.* **1998**, *80*, 4249−4252.
(17) Averitt, R. D.; Westcott, S. L.; Halas, N. J. *Phys. Rev. B* **1998**, *58*, R10203−R10206.
(18) Link, S.; Hathcock, D. J.; Nikoobakht, B.; El-Sayed, M. A. *Adv. Mater.* **2003**, *15*, 393.
(19) Link, S.; Burda, C.; Nikoobakht, B.; El-Sayed, M. A. *J. Phys. Chem. B* **2000**, *104*, 6152−6163.
(20) Radloff, C.; Halas, N. J. *Appl. Phys. Lett.* **2001**, *79*, 674−676.
(21) Kamat, P. V.; Flumiani, M.; Hartland, G. V. *J. Phys. Chem. B* **1998**, *102*, 3123−3128.
(22) Kurita, H.; Takami, A.; Koda, S. *Appl. Phys. Lett.* **1998**, *72*, 789−791.
(23) Mafune, F.; Kohno, J.; Takeda, Y.; Kondow, T. *J. Phys. Chem. B* **2001**, *105*, 9050−9056.
(24) Bosbach, J.; Martin, D.; Stietz, F.; Wenzel, T.; Trager, F. *Appl. Phys. Lett.* **1999**, *74*, 2605−2607.
(25) Chang, S. S.; Shih, C. W.; Chen, C. D.; Lai, W. C.; Wang, C. R. C. *Langmuir* **1999**, *15*, 701−709.
(26) Link, S.; El-Sayed, M. A. *J. Chem. Phys.* **2001**, *114*, 2362−2368.
(27) Prodan, E.; Nordlander, P.; Halas, N. J. *Chem. Phys. Lett.* **2002**, *368*, 94.
(28) Prodan, E.; Nordlander, P. *Nano Lett.* **2003**, *3*, 543−547.
(29) Prodan, E.; Nordlander, P. *Chem. Phys. Lett.* **2002**, *352*, 140−146.
(30) Oldenburg, S. J.; Westcott, S. L.; Averitt, R. D.; Halas, N. J. *J. Chem. Phys.* **1999**, *111*, 4729−4735.
(31) Sun, Y.; Xia, Y. *Anal. Chem.* **2002**, *74*, 5297−5305.
(32) Tam, F.; Halas, N. J. *Prog. Org. Coat.*, in press.
(33) Sershen, S. R.; Westcott, S. L.; Halas, N. J.; West, J. L. *J. Biomed. Mater. Res.* **2000**, *51*, 293−298.
(34) Hirsch, L. R.; Jackson, J. B.; Lee, A.; Halas, N. J.; West, J. *Anal. Chem.* **2003**, *75*, 2377−2381.
(35) Hirsch, L. R.; Stafford, R. J.; Bankson, J. A.; Sershen, S. R.; Price, R. E.; Hazle, J. D.; Halas, N. J.; West, J. L. *Proc. Natl. Acad. Sci. U.S.A.* **2003**, *100*, 13549−13554.
(36) Stober, W.; Fink, A.; Bohn, E. *J. Colloid Interface Sci.* **1968**, *26*, 62−69.
(37) Duff, D. G.; Baiker, A. *Prep. Catal. VI: Proc. Int. Symp., 6th, 1994* **1995**, *91*, 505−512.
(38) Lenzner, M.; Krüger, J.; Kautek, W.; Krausz, F. *Appl. Phys. A* **1999**, 465−466.
(39) Hu, M.; Wang, X.; Hartland, G. V.; Mulvaney, P.; Juste, J. P.; Sader, J. E. *J. Am. Chem. Soc.* **2003**, *125*, 14925−14933.
(40) Westcott, S. L.; Averitt, R. D.; Wolfgang, J. A.; Nordlander, P.; Halas, N. J. *J. Phys. Chem. B* **2001**, *105*, 9913−9917.
(41) Mohamed, M. B.; Ismail, K. Z.; Link, S.; El-Sayed, M. A. *J. Phys. Chem. B* **1998**, *102*, 9370−9374.
(42) Pitsillides, C. M.; Joe, E. K.; Wei, X. B.; Anderson, R. R.; Lin, C. P. *Biophys. J.* **2003**, *84*, 4023−4032.
(43) Huttmann, G.; Birngruber, R. *IEEE J. Sel. Top. Quantum Electron.* **1999**, *5*, 954−962.